CYP26A1 Links WNT and Retinoic Acid Signaling: A Target to Differentiate ALDH+ Stem Cells in APC-Mutant CRC

Caroline O. B. Facey , Victoria Oluwajuwon Hunsu , Chi Zhang , Brian Osmond , Lynn Opdenaker , Bruce Boman *

Posted Date: 18 December 2023

doi: 10.20944/preprints202312.1224.v1

Keywords: CYP26A1; colorectal cancer; cancer stem cells; APC; aldehyde dehydrogenase; WNT; retinoic acid; enteroendocrine cells

Article

CYP26A1 Links WNT and Retinoic Acid Signaling: A Target to Differentiate ALDH+ Stem Cells in *APC*-Mutant CRC

Caroline O. B. Facey [1], Victoria O. Hunsu [1,2,†], Chi Zhang [1,2,†], Brian Osmond [1,2], Lynn M. Opdenaker [1] and Bruce M. Boman [1,2,3,*]

1. Cawley Center for Translational Cancer Research, Helen F. Graham Cancer Center and Research Institute, Newark, DE; Caroline.Facey@christianacare.org, LOpdenaker@christianacare.org
2. Dept Biological Sciences, University of Delaware, Newark, DE; vhunsu@udel.edu, johnitch@udel.edu, bosmond@udel.edu
3. Dept Pharmacology & Experimental Therapeutics, Thomas Jefferson University, Philadelphia PA

* Correspondence: author: Bruce M. Boman, MD, PhD; Tel: 267-303-9241 Email: brboman@udel.edu

† Contributed equally to this project.

Simple Summary: This manuscript reports discovery of a mechanism that links two major cellular pathways, retinoic acid and WNT signaling, which are involved in colorectal cancer development.

Abstract: *APC* mutation is the main driver mechanism of CRC development and leads to constitutively activated WNT signaling, overpopulation of ALDH+ stem cells (SCs), and incomplete differentiation. We previously reported that retinoic acid (RA) receptors are selectively expressed in ALDH+ SCs, which provides a way to target cancer SCs with retinoids to induce differentiation. *Hypotheses*: A functional link exists between WNT and RA pathways, and *APC* mutation generates a WNT:RA imbalance that decreases retinoid-induced differentiation and increases ALDH+ SCs. Accordingly, to restore parity in WNT:RA signaling, we induced *wt-APC* expression in *APC*-mutant CRC cells and assessed the ability of all-trans-retinoic acid (ATRA) to induce differentiation. Notably, ATRA substantially increased expression of the WNT-target gene, *CYP26A1*, and inducing *wt-APC* reduced this expression by 50%. Thus, RA and WNT pathways crosstalk to modulate CYP26A1 metabolism of retinoids. We found that inducing *wt-APC* augments ATRA-induced cell differentiation by: i) decreasing cell proliferation; ii) suppressing *ALDH1A1* expression; iii) decreasing ALDH+ SCs; iv) increasing neuroendocrine cell differentiation. Furthermore, NanoString profiling/bioinformatics identified a novel CYP26A1-based network that links WNT and RA signaling. Moreover, *CYP26A1* inhibitors sensitized CRC cells to the anti-proliferative effect of drugs that downregulate WNT signaling. Notably. in *wt-APC*-CRCs, decreased CYP26A1 improves patient survival. These findings have strong potential for clinical translation.

Keywords: *CYP26A1*; colorectal cancer; cancer stem cells; *APC*; aldehyde dehydrogenase; WNT; retinoic acid; enteroendocrine cells

1. Introduction

Our goal has been to understand how mutation in the *APC* gene causes overpopulation of aldehyde dehydrogenase-positive (ALDH+) cancer SCs (CSCs) and decreased differentiation of SCs into neuroendocrine cells (NECs). The *APC* tumor suppressor gene is a negative regulator of WNT-signaling, which controls SC population size [1,2]. ALDH is a key enzyme in retinoic acid (RA) signaling, which is a pathway that promotes SC differentiation [3–7]. Thus, we chose to investigate whether there is a functional connection between WNT and RA signaling, and if *APC* mutation generates an imbalance in a WNT:RA-linked mechanism that contributes to ALDH+ SC overpopulation by impeding retinoid-induced differentiation [8].

 doi:10.20944/preprints202312.1224.v1

We previously reported that inducing *wild type (wt)-APC* in HT29 CRC cells, which contain homozygous mutant *APC*, leads to decreased cell proliferation and increased apoptosis [9–11]. In mice, inactivation of *APC* leads to intestinal adenoma formation which provided evidence for crypt SCs as the cells-of-origin of intestinal cancer [12,13]. Restoring *Apc* in murine tumors led to increased enterocyte differentiation, tumor regression, and re-established crypt-villus homeostasis in CRC [13].

Previously we found that RA receptors are selectively expressed in ALDH+ SCs, which indicates RA signaling mainly occurs in ALDH+ SCs [14]. Since ALDH is a key enzyme in the RA pathway and RA signaling occurs via ALDH+ SCs, it provides a mechanism to selectively target CSCs based on a therapeutic strategy involving retinoid-induced differentiation [15]. Indeed, retinoids have been previously studied as chemo-preventive drugs and systemic therapies in treatment of CRC and other cancers [16,17]. Furthermore, we found that RA ligands such as ATRA induce differentiation of ALDH+ SCs into NECs [8,18]. On the other hand, *APC* mutation leads to incomplete differentiation in CRC cells [8,19]. Altogether, these findings suggest that *APC* mutation attenuates RA signaling in ALDH+ SCs, which contributes to their overpopulation that drives CRC development [8].

To identify mechanisms that functionally link WNT and RA signaling, we investigated how inducing *wt-APC* expression to decrease WNT signaling affects ATRA's ability to induce NEC differentiation and reduce ALDH+ CSCs in *APC* mutant CRC.

2. Materials and Methods

2.1. Cell Culture and Inducing wt-APC Expression

HT29 colon carcinoma cells containing a ZnCl2-inducible *wt-APC* or β-galactosidase (control) expression vector were provided by Dr. Bert Vogelstein's lab (Johns Hopkins University) [9] We refer to the modified HT29 cells as HT29-APC or HT29-GAL cells. HT29 cells were chosen for most of the study because they contain a homozygous *APC* mutation and do not have any known retinoic acid receptor gene mutations. Modified cells were cultivated in McCoy's 5A modified media (Gibco/Thermofisher Scientific) supplemented with 10% fetal bovine serum (FBS; Atlanta Biologicals/R&D Systems), 1% penicillin:streptomycin (pen-strep; VWR), and 600 µg/mL hygromycin B (Thermofisher Scientific). All variations of HT29 cells grew equally well in terms of cell density. Respective expression plasmids were induced with 120 µM ZnCl2 (Sigma-Aldrich) for the times indicated. HT29-APC cells treated with $ZnCl_2$ are referred to *wt-APC* and those not treated with $ZnCl_2$ are referred to mt-*APC*. All cells were maintained in a 37°C incubator with 5% CO2.

2.2. Cell Proliferation

HT29 cells were plated at 12,000 cells per well into 96-well plates. Cells were allowed to adhere for 24 hrs and serum-starved for an additional 24 hrs. Cells were then treated for 48 hrs with $ZnCl_2$ and/or ATRA (Stem Cell Technologies) as indicated. Controls involved no ZnCl2 or DMSO (0.1%; Fisher Scientific) vehicle. After indicated time, cells were washed in PBS and stained in 0.5% crystal violet (Sigma-Aldrich) solution for 20 minutes. Excess crystal violet was then washed off with deionized water and left to dry at room temperature for at least 24 hrs. Dried crystal violet stain was then re-suspended in 10% acetic acid solution and optical density measured at 570 nm using a Tecan Multi-Plate Reader, data was quantified using Tecan i-Control software, and analyzed using Microsoft Excel. Values reflect cell proliferation as our standard curve shows that absorbance values from crystal violet staining are directly proportional to cell number. The proliferation index is calculated by normalizing cell proliferation index of treated to untreated cells. Biological replicates were performed in triplicate with 6 technical replicates per condition, and the average plotted with standard error of the mean (SEM) indicated.

2.3. WNT/β-Catenin Activity

WNT/β-catenin activity was measured using the TCF/LEF Reporter (BPS Biosciences) and Two-Step or Dual Glo (Firefly and Renilla) Luciferase Assays (BPS Biosciences or Promega) according to manufacturer instructions. In brief, cells were plated onto clear bottom, white 96-well plates and

 doi:10.20944/preprints202312.1224.v1

adhered for 24 hrs. Next, cells were transfected with the TCF/LEF reporter plasmids using Lipofectamine 3000 (Thermofisher Scientific). Cells were then treated as indicated for 24 hrs. The Firefly and Renilla luciferase assays were performed, and luminescence recorded using a Tecan Multi-Plate Reader, i-Control software, and data analyzed using Microsoft Excel. Luciferase activity was measured by calculating the ratio of Firefly to Renilla luminescence signals. Biological replicates were performed in triplicate and with 6 technical replicates per condition. The average luciferase activity was plotted with SEM indicated.

2.4. NanoString Profiling

To measure the effects of manipulating WNT and RA signaling, we utilized the nCounter PanCancer Pathways Panel from NanoString to provide high-throughput data including differential gene expression and subsequent pathway analysis. The PanCancer Pathways Panel includes 770 genes involved in several cancer pathways including WNT, hedgehog, apoptosis, cell cycle, RAS, PI3K, STAT, MAPK, Notch, TGF-β, chromatin modification, transcriptional regulation, and DNA damage control [20] and we included an additional 55 genes of interest to evaluate SC marker, differentiation marker, ALDH isoforms, RA receptors, and HOX genes.

HT29-*APC* cells were plated at 700,000 cells per well onto 6-well plates and allowed to adhere for 24 hrs. Cells were then serum-starved for 24 hrs. Cells were then treated with 15 μM ATRA or 0.1% DMSO and 120 μM $ZnCl_2$ or no $ZnCl_2$ for 24 hrs. Total RNA was isolated from cell lysates using the Trizol method. Samples were frozen at -80°C and sent to Wistar Institute's Genomic Core Facility for analyzing quality of RNA and subsequent NanoString profiling using the Pan-cancer Panel. Results were obtained in RCC file format and data analyzed using NanoString nSolver software. A heat map was then generated to show differential expression of 785 mRNAs amongst the four treatment conditions (+$ZnCl_2$ & +ATRA, + $ZnCl_2$ & -ATRA, - $ZnCl_2$ & +ATRA, $ZnCl_2$ & -ATRA). Ratios were determined using nSolver, significance assessed, and plotted in Microsoft Excel. Gene lists of interest were analyzed using the STRING database for protein-protein interaction networks and functional enrichment [21].

2.5. Western Blotting & Densitometry

Standard western blotting procedures were performed. Cells were plated, treated as indicated with 120 μM ZnCl2 (Millipore Sigma), ATRA, or DMSO and lysed with RIPA (Millipore Sigma) containing Halt Protease and Phosphatase Inhibitor (Thermofisher) and cysteine protease inhibitor E-64 (Millipore Sigma). Cells lysates were scraped from dishes and centrifuged at 12,000 rpm for 15 minutes and stored at -20°C. Protein concentrations were determined using the Pierce BCA Protein Assay Kit (Thermofisher) and 100 μg total protein was prepared in Laemmli buffer (Bio-Rad) and 2.5% or 5% β-mercaptoethanol (Bio-Rad). Samples were loaded onto 4-20% mini-precast gradient gels (Bio-Rad) for SDS-PAGE at 200V for 45 minutes. Proteins were then transferred to PVDF membrane (Thermofisher) at 90V for 2 hrs. Blots were then blocked in 5% BLOTTO (nonfat dried milk in tris buffered saline (TBS) with 0.1% Tween 20 [TBST]) for 1 hr. Next, blots were incubated in primary antibody prepared in BLOTTO overnight on a rocking platform at 4°C. Blots were then washed in TBST 3x for 10 minutes. Secondary antibody was prepared in BLOTTO and blots incubated for 1-2 hrs at room temperature. Blots were then washed in TBST 3x for 10 min and incubated in Super Signal West Dura Extended Duration Substrate (Thermofisher) for 5 minutes to detect horseradish peroxidase conjugation. Blots were then imaged using the LiCor Odyssey Fc developer and Image Studio software. Densitometry was done using Image Studio and graphs plotted using Microsoft Excel. Experiments were performed 3 times and standard error of the mean (SEM) was calculated and plotted as shown.

2.6. Flow Cytometry and Fluorescence Activated Cell Sorting

NEC and ALDH+ (ALDEFLUOR+) cells were quantified and/or isolated using GLP2R antibody conjugated to Alexafluor 594 (Novus Biologicals) with IgG control (R&D) or ALDEFLUOR Assay

 doi:10.20944/preprints202312.1224.v1

(Stem Cell Technologies) using manufacturer's instructions. Flow cytometry was performed on a BD FACS Aria II and FACS performed on a BD LSR Fortessa. Data was processed using FACS Diva software and graphs plotted in Microsoft Excel with error bars indicating SEM. Experiments were done 3 times.

2.7. Determining synergistic, Additive, or Antagonistic Anti-Proliferative Effects of CYP26A1 and WNT Signaling Inhibitors

We investigated the anti-proliferative effects of the *CYP26A1* inhibitors Liarozole and Talarozole in combination with agents (Sulindac or Piroxicam) that have anti-tumor activity against *APC*-mutant tissues [reviewed in 16]. HT29 and HCT116 cells were cultivated in McCoy's 5A media supplemented with 10% FBS and 1% pen-strep. SW480 cells were cultivated in Leibovitz L15 media supplemented with 10% FBS and 1% pen-strep. Cells were plated, allowed to adhere for 24 hrs, and serum-starved for 24 hrs. The cells were then treated for 48 hrs with the various agents as single drugs or in combination. For *CYP26A1* inhibitors, IC50 doses of Liarozole and Talarozole are as follows: HT29 cells- 80 and 30 μM, HCT116 cells- 110 and 22 μM, and SW480 cells- 80 and 25 μM, respectively. For WNT inhibitors, IC50 doses of Sulindac and Piroxicam are as follows: HT29 cells- 680 μM and 550 μM, HCT116 cells- 450 μM and 600 μM, SW480 cells- 220 μM and 270 μM, respectively. In dose response experiments, Sulindac and Piroxicam doses were varied based on the IC50 dose (75% of IC50, IC50, 125% of IC50). For clarity, all concentrations are listed in Table S2. The proliferation index was determined using crystal violet assay (see above). Synergistic, additive, or antagonistic effects were calculated based on the Bliss independence dose-response model [22]. For example, these effects were calculated as the ratio of observed (observed values for the combination of drug a & b) divided by predicted (values for individual drug a multiplied by individual values for drug b), based on the Bliss Independence dose-response model. Further analyses were performed as described in main and supplementary figure legends.

2.8. Patient Survival Studies

RNA-seq, genotype, and clinical data on CRC patients were obtained from Genomic Data Commons (GDC) data portal. For individual patients, records of their *APC* genotypes, survival data, as well as *CYP26A1* expression in both human CRC and normal human colon samples were paired together. These patients were then grouped based on whether they carry *APC* mutation and the change (either increase or decrease) of *CYP26A1* expression between CRC and normal colon tissue samples.

2.9. Statistical Analyses

Statistics were calculated either in Excel using the t-test function or GraphPad Prism using one-way ANOVA, two-way ANOVA, or multiple unpaired t-tests as indicated in the figure legends. For patient survival studies, Kaplan-Meier survival curves of different groups were compared using log-rank tests.

3. Results

3.1. Inducing wt-APC Decreases WNT Signaling and Reduces Expression of WNT Target Genes

We first wanted to show that the HT29-*APC* cell line established by Morin et al [9] was functioning correctly in the ability of $ZnCl_2$-treatment to induce *wt-APC* expression. Using two independent experimental approaches, we confirmed that expression of *wt-APC* occurs in response to $ZnCl_2$ treatment (Figure S1). We initially measured WNT activity utilizing the TopFlash luciferase reporter assay which measures TCF/LEF transcriptional activity. There was a 90% reduction in WNT activity in $ZnCl_2$-treated cells compared to untreated cells (Figure S1A). We then confirmed that reduced expression occurs in several proteins encoded by WNT/ β-catenin target genes [23] including MET [24], c-JUN [25], CD44 [26], and c-MYC [27] (Figure S1B).

Preprints (www.preprints.org) | NOT PEER-REVIEWED | Posted: 18 December 2023 doi:10.20944/preprints202312.1224.v1

3.2. ATRA Promotes WNT/β-Catenin Activity, wt-APC Attenuates ATRA's Effect

Although ATRA reduces the number of ALDH+ SCs, reduces sphere-forming ability, and promotes differentiation of SCs in CRC [14], here we found that total cell proliferation in cells is reduced less than 20% at 48 hrs when treated with 20 μM ATRA (Figure 1A). However, when *wt-APC* expression was induced in HT29 cells, ATRA led to further reduction of total cell proliferation by 42% compared to untreated controls (Figure 1A). Dose response analysis also shows that cells with *wt-APC* are 2.4 times more responsive to the anti-proliferative effects of ATRA than cells with mt-*APC* (based on line slopes; Figure 1B). Additionally, we observed that WNT/β-catenin activity is increased by ATRA in HT29 cells by up to 10 times as compared to control (Figure 1C); but, this increase in WNT activity is attenuated with the expression of *wt-APC* (Figure 1C).

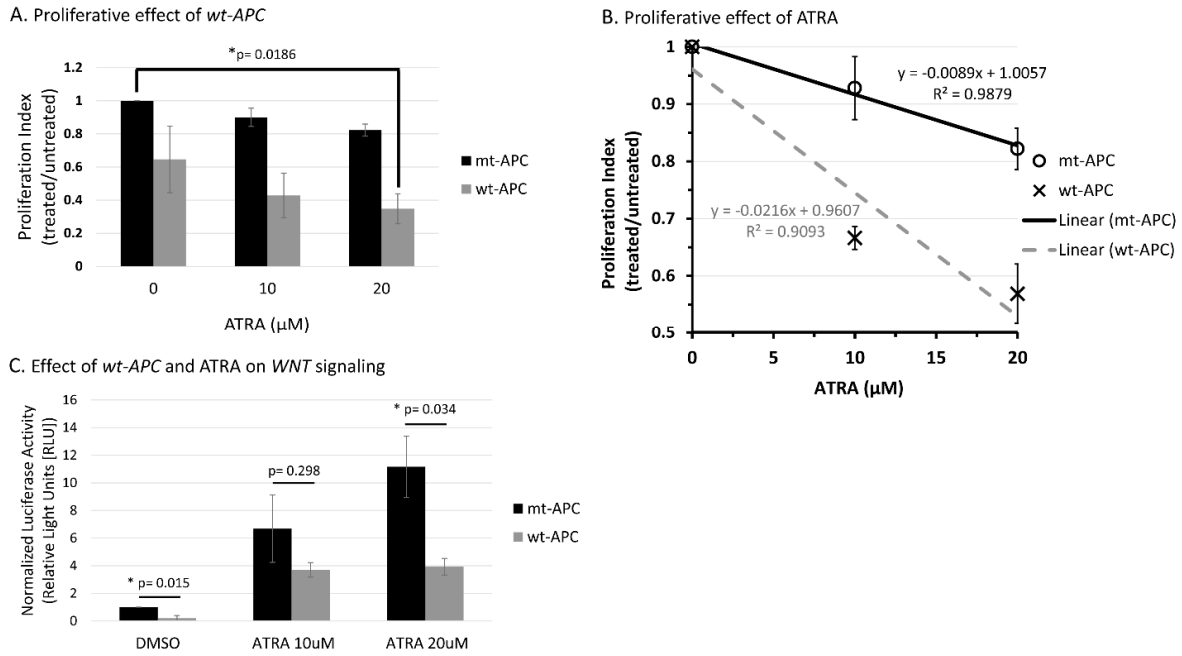

Figure 1. *Wt-APC* expression sensitizes HT29 cells to ATRA's ability to decrease cell proliferation and attenuates ATRA-induced WNT/β- catenin activity. A) Cell proliferation was reduced by 65% when *wt-APC* was induced by $ZnCl_2$ and cells were treated with 20 μM ATRA for 48hrs. Values are normalized to *mt-APC* DMSO control. B) Cell proliferation was reduced by approximately 10% (10 μM) and 20% (20 μM) in mutant-*APC* (*mt-APC*) cells (black line). Cell proliferation was further reduced by approximately 36% (10 μM) and 42% (20 μM) in wildtype-*APC* (*wt-APC*) cells (dashed gray line). Similar results were seen at 24hrs, altogether indicating a time- and concentration-dependent effect. *Mt-APC* and *wt-APC* values were normalized to each of their respective DMSO controls. C) TCF/LEF Reporter Assay was performed to determine WNT/β- catenin activity. ATRA caused an increase in WNT- activity in mt-*APC* cells (black bars) however, this increase was partially attenuated when *wt-APC* expression was induced (gray bars). Experiments (n=3) were performed with error bars plotted as standard error of the mean (SEM). Multiple unpaired t-tests determined statistical significance where p=<0.05.

3.3. Inducing wt-APC Decreases ALDH+ Stem Cells and Increases NEC Differentiation

Here, we show an increase in the percentage of GLP2R+ NECs when *wt-APC* expression is induced (Figure 2A). The relative number of GLP2R+ cells quadruples when *wt-APC* is induced and increases 6-fold with combined *wt-APC* expression and ATRA as compared to mt-*APC* and no ATRA (Figure 2B). In parallel, the percentage of ALDH+ (ALDEFLUOR+) cells decreases by approximately 20% with ATRA alone and almost 60% with the combination of ATRA treatment and *wt-APC* induction (Figure 2C). In a similar manner, mRNA expression of *ALDH1A1* decreased by 5-fold with

Preprints (www.preprints.org) | NOT PEER-REVIEWED | Posted: 18 December 2023 doi:10.20944/preprints202312.1224.v1

the ATRA and *wt-APC* combination as compared to control (Figure 2D). These results further support the existence of an interplay between the WNT and RA signaling pathways.

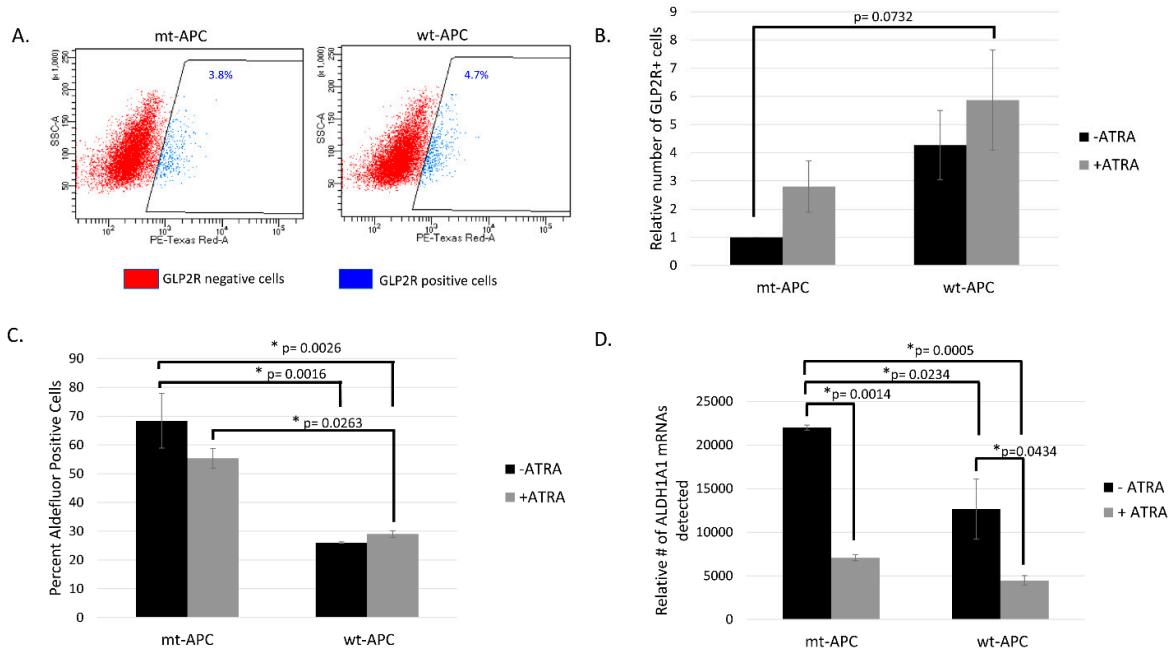

Figure 2. Inducing *wt-APC* enhances differentiation of neuroendocrine cells: GLP2R + cells increase and ALDH+ cells decrease. A) GLP2R+ and GLP2R- cells were sorted from parent HT29 cells (mt-*APC*) and from cells induced to express *wt-APC*. The percentage of GLP2R+ subpopulation is shown. B) Cells were stained for GLP2R, and relative number calculated by normalizing to untreated mt-*APC* cells. The relative number of GLP2R+ cells quadruple when *wt-APC* is induced (black bars) and increases by 6-fold with the combination of *wt-APC* and ATRA (comparing mt-*APC* black bar and *wt-APC* gray bar). C) The percentage of ALDH+ SCs cells decreased by ~20% with ATRA alone and up to ~60% when HT29 cells were induced to express *wt- APC*. D) Results from NanoString profiling show a similar decrease in *ALDH1A1* mRNA in response to ATRA and *wt-APC*. Experiments were performed 3 times and statistical significance was determined by two-way ANOVA with multiple comparisons.

We also investigated whether inducing *wt-APC* in HT29-*APC* cells changes the expression of NEC differentiation cell markers. Indeed, several NEC markers increase in expression with the expression of *wt-APC* in HT29 cells. Increased protein expression of CHGA, GLP2R, NSE (ENO2), and SSTR1 occurred as shown in (Figure 3). Overall, we found that inducing *wt-APC* in cells decreases ALDH+ CSCs and increases NEC differentiation.

Preprints (www.preprints.org) | NOT PEER-REVIEWED | Posted: 18 December 2023 doi:10.20944/preprints202312.1224.v1

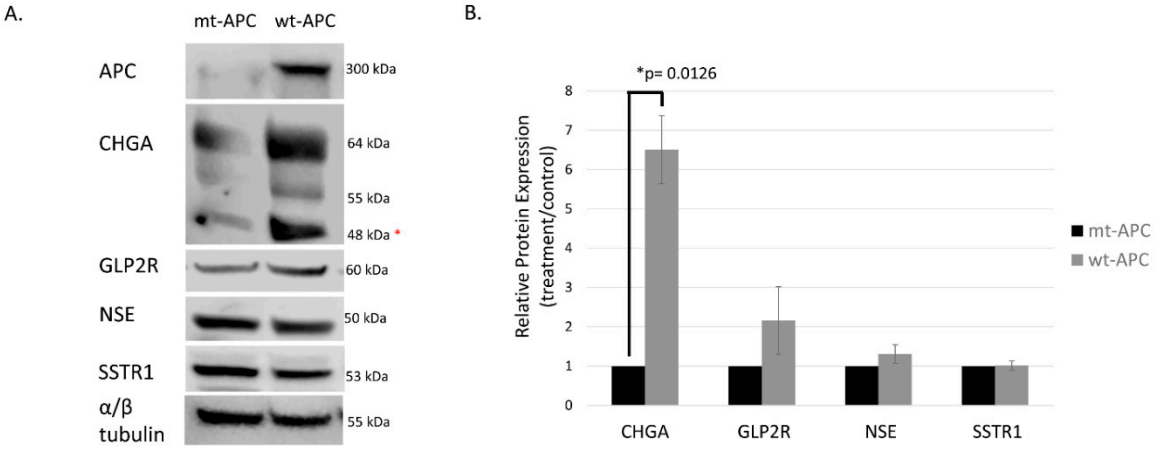

Figure 3. Protein expression of neuroendocrine markers is increased with induction of *wt-APC*. HT29 cells were induced to express *wt-APC*. Western blot (A) and densitometry (B) were performed to analyze protein expression of neuroendocrine markers. Expression of full- length *APC* is shown and verified in the top right panel of (A). Chromogranin A (CHGA), GLP2R, and NSE/ enolase are increased with *wt-APC* but, SSTR1 is increased to a lesser extent. *The lower CHGA band was analyzed for densitometry, higher bands may indicate post-translational modification such as glycosylation of the protein. The experiment (n=3) was performed with averages plotted in (B) and representative blot in (A). Statistical significance was determined by multiple unpaired t-tests.

3.4. Expression Profiling Identified CYP26A1 as a Link between WNT and RA Signaling Pathways

NanoString profiling revealed differential expression of 785 mRNAs across four treatment groups from results on $ZnCl_2$ to induce *wt-APC* expression and ATRA to increase RA signaling (+$ZnCl_2$ & +ATRA, +$ZnCl_2$ & -ATRA, -$ZnCl_2$ & +ATRA, -$ZnCl_2$ & -ATRA). Hierarchical, agglomerative clustering was achieved and shown as a heat map that was generated using nSolver software (Figure 4A).

To examine the effect of inducing *wt-APC* expression and increasing RA signaling at the same time, we calculated the ratio of treated cells (+$ZnCl_2$ & +ATRA) to corresponding control group (-$ZnCl_2$ & -ATRA) using the nSolver software. A set of 248 genes was identified as being differentially expressed (Figure S2). To identify predicted signaling pathway interactions, we analyzed the set of 248 genes using the STRING database [21]. The large number of predicted interactions found in this network analysis (Figure S2) suggests that a substantial level of crosstalk occurs when the WNT and RA signaling pathways are modulated in HT29 cells.

By analyzing the list of 248 genes using the DAVID functional tool [29] and ranking the list of over 1500 hits, we identified those genes that are involved in RA signaling using the GOTERM_BP_DIRECT list. We then re-analyzed this list of 14 genes using the STRING database and found several predicted interactions. Of the 14 genes listed as involved in RA signaling, 12 were identified to have protein interactions: CYP26A1, RARA, HDAC2, KLF4, TNF, LEP, PDGFA, MYB, DKK1, WNT7B, WNT11, and FZD7 (Figure 4B). Notably, five WNT target genes were identified: CYP26A1 [30], WNT7B, WNT11, FZD7, and DKK1 (listed on NanoString's Gene to Pathway Summary). However, CDKN2D and HOXA2 did not show any predicted connections with the other proteins identified in our current STRING network.

The highest change in expression occurred in *CYP26A1* with a 15.52-fold increase when both *wt-APC* expression is induced and cells are treated with ATRA (Figure 4C). Moreover, HT29 cells treated with ATRA alone experience a 30.8-fold increase in *CYP26A1* expression and inducing *wt-APC* attenuates this increase by 50% (Figure 5A). Western blot experiments validated the 50% decrease in *CYP26A1* expression when cells are induced to express *wt-APC* and treated with 20 μM ATRA (Figure 5B,C).

Preprints (www.preprints.org) | NOT PEER-REVIEWED | Posted: 18 December 2023 doi:10.20944/preprints202312.1224.v1

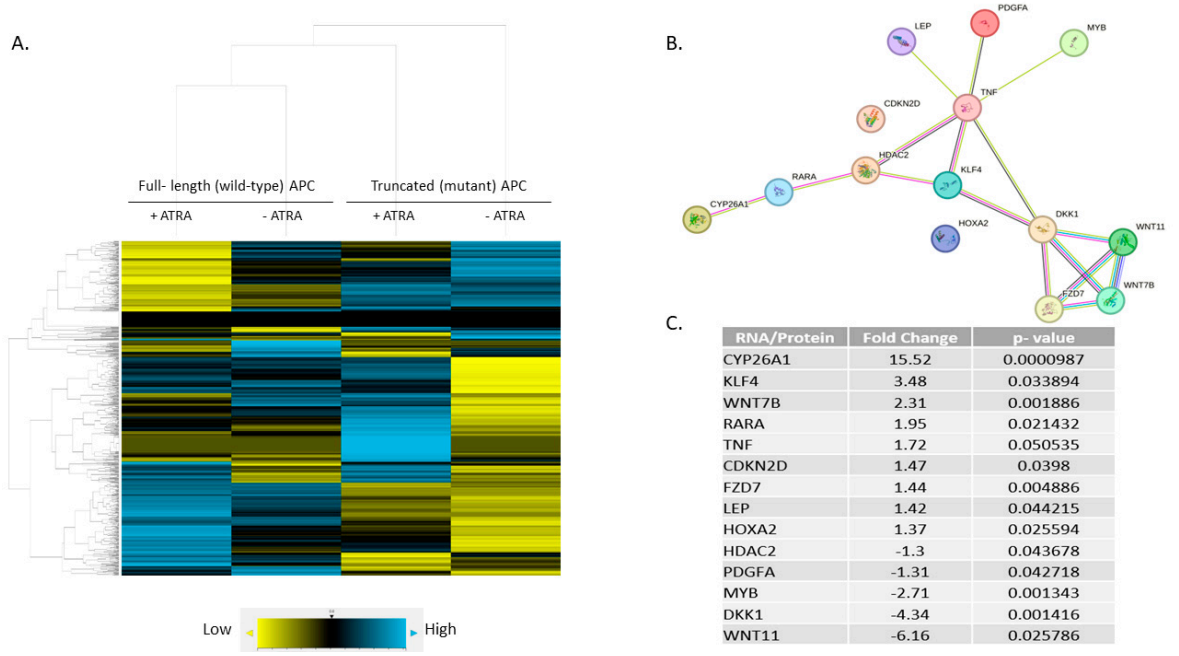

C.

RNA/Protein	Fold Change	p- value
CYP26A1	15.52	0.0000987
KLF4	3.48	0.033894
WNT7B	2.31	0.001886
RARA	1.95	0.021432
TNF	1.72	0.050535
CDKN2D	1.47	0.0398
FZD7	1.44	0.004886
LEP	1.42	0.044215
HOXA2	1.37	0.025594
HDAC2	-1.3	0.043678
PDGFA	-1.31	0.042718
MYB	-2.71	0.001343
DKK1	-4.34	0.001416
WNT11	-6.16	0.025786

Figure 4. A predicted protein network linking RA and WNT pathways. A) Hierarchical, agglomerative clustering using NanoString nSolver software generated a heatmap showing differential expression of 785 mRNAs amongst four treatment conditions. Yellow = low expression, blue = high expression, black = negligible expression at or below background level. B) A subset of 248 genes was identified with significant fold-change in expression between *wt-APC* + ATRA versus mt-*APC* -ATRA (Figure S2). DAVID analysis identified a list of 14 genes involved in cellular response to RA. STRING software analysis of the 14 genes (C) identified network interactions (B).

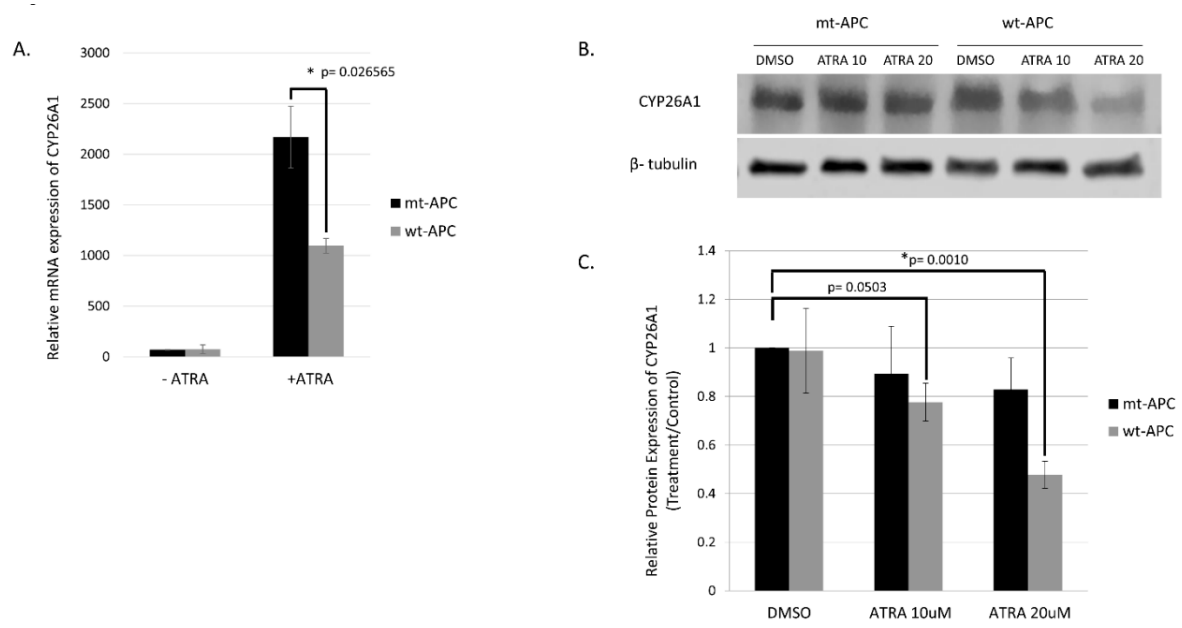

Figure 5. Inducing *wt-APC* expression reduces ATRA induced *CYP26A1* expression. (A) NanoString mRNA profiling and western blot analysis of protein expression (B, C) revealed a 50% decrease in *CYP26A1* expression when *wt-APC* expression was induced in ATRA-treated HT29 cells. Experiments were performed in triplicate and a representative blot is shown in (B). Statistical significance was determined by multiple unpaired t-test (A) and one-way ANOVA (C).

Preprints (www.preprints.org) | NOT PEER-REVIEWED | Posted: 18 December 2023 doi:10.20944/preprints202312.1224.v1

3.5. CYP26A1 Inhibitor Agents Sensitize CRC Cells to the Anti-Proliferative Effect of Drugs That Downregulate WNT Signaling.

The anti-proliferative effects of CYP26A1 inhibitors, Liarozole and Talarozole, were evaluated alone and in combination with drugs that downregulate WNT signaling, Piroxicam and Sulindac (Figures 6 and S3). Three CRC cell lines with mutations that activate WNT signaling were used, two with mutant *APC* (HT29 & SW480) and one with mutant β-catenin/*CTNNB1* (HCT116). Each of the three cell lines have different RA receptor genotypes. HT29 cells have wild-type retinoid receptors, SW480 cells have mutations in RARA and RXRG, and HCT116 cells have mutant RARA [16]. Sulindac and Piroxicam have anti-tumor activity against *APC* mutant tissues, and Sulindac has been shown to target β-catenin and downregulate WNT signaling [reviewed in 16].

CRC cells were treated with the various agents as single drugs or in combination (Figures 6 and S3). The Sulindac and Piroxicam doses were varied based on the IC50 (half-maximal inhibitory concentration) dose for treated cell lines. The data reveal that anti-tumor agents Sulindac and Piroxicam decrease the proliferation of CRC cells. The data also shows that the CYP26A1 inhibitors Liarozole and Talarozole alone reduce CRC proliferation. Moreover, when Sulindac or Piroxicam was combined with Liarozole or Talarozole, the drug combination produced additive or synergistic effects (Figure 6C,F). Further dose response analysis on the anti-proliferative effects of varying Piroxicam and Sulindac concentrations showed that Liarozole & Piroxicam, Liarozole & Sulindac, and Talarozole & Sulindac combinations produced the highest dose responsiveness in HT29, SW480, and HCT116 cells, respectively (Figure S4A,B).

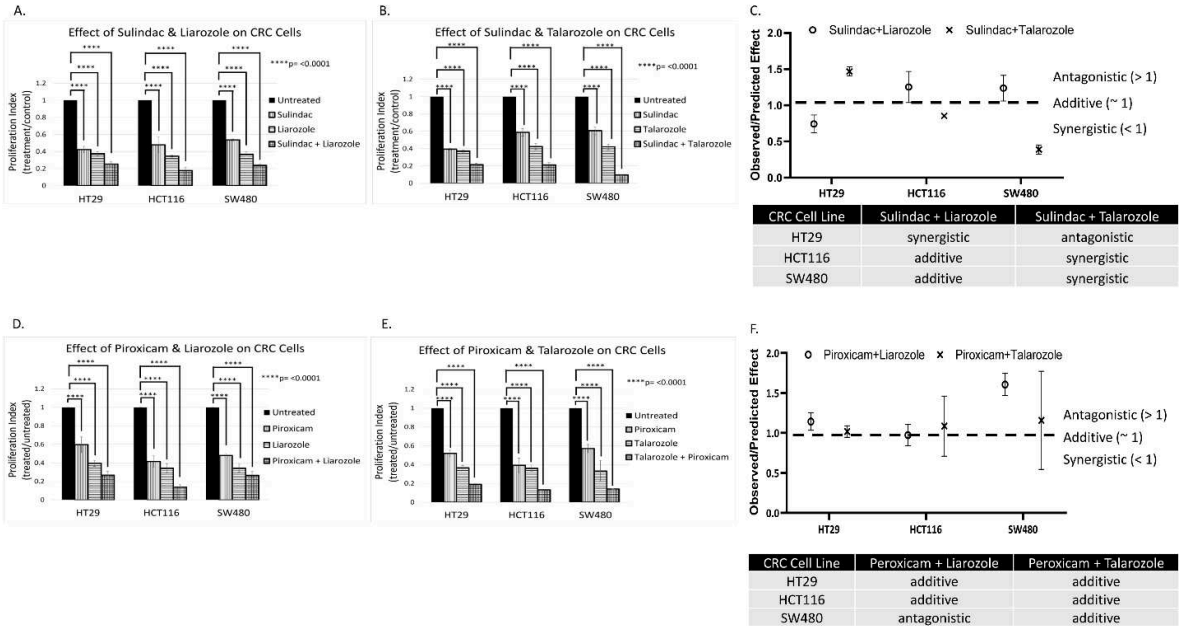

CRC Cell Line	Sulindac + Liarozole	Sulindac + Talarozole
HT29	synergistic	antagonistic
HCT116	additive	synergistic
SW480	additive	synergistic

CRC Cell Line	Peroxicam + Liarozole	Peroxicam + Talarozole
HT29	additive	additive
HCT116	additive	additive
SW480	antagonistic	additive

Figure 6. Effect of *CYP26A1* inhibitor and WNT inhibitor drug combinations on HT29, HCT116, and SW480 CRC cells. Panels A, B, D, and E show that anti-tumor agents Sulindac and Piroxicam alone decrease the proliferation of the CRC cell lines having mt-*APC*. The data also shows that the *CYP26A1* inhibitors Liarozole and Talarozole alone reduce CRC proliferation. Panels C and F shows that when Sulindac or Piroxicam was combined with Liarozole or Talarozole, the drug combination produced additive or synergistic effects. These effects were calculated as the ratio of observed divided by predicted response (see methodes) based on the Bliss Independence dose-response model [22]. Statistical significance was determined by two-way ANOVA. Extended data showing additional concentrations are shown in Figure S3 and concentrations listed in Table S2.

Preprints (www.preprints.org) | NOT PEER-REVIEWED | Posted: 18 December 2023 doi:10.20944/preprints202312.1224.v1

3.6. Analysis of Human CRC Cases Indicates CYP26A1 Predicts Survival of Patients with Wild-type APC Tumors

To evaluate the effects of *CYP26A1* on CRC patient survival, we conducted multi-omics bioinformatics analysis using RNA-seq, mutation, and clinical data obtained from Genomic Data Commons (GDC). Patients were grouped based on their *APC* genotypes and changes (increase or decrease) of *CYP26A1* expression level between CRC and normal human colon samples. We found that the majority of CRC patients express increased levels of *CYP26A1* in their CRC samples compared to normal colon tissue from the same patient, and this difference is statistically significant (Figure 7A). By itself, this change in *CYP26A1* expression level is not a statistically significant predictor of patient survival (Figure 7B). However, when genotype of *APC* was used to further sub-group the patients, we found that *CYP26A1* expression is a significant predictor of patient survival only when patient tumors are *wild-type APC* (Figure 7C). But estimated survival is not statistically significant between increased and decreased *CYP26A1* expression groups among those patient tumors carrying *APC* mutations (Figure 7D). Similarly, when patients are sub-grouped based on *CYP26A1* level, *APC* mutation is not a significant predictor of patient survival (Supplementary Figure 7A,B).

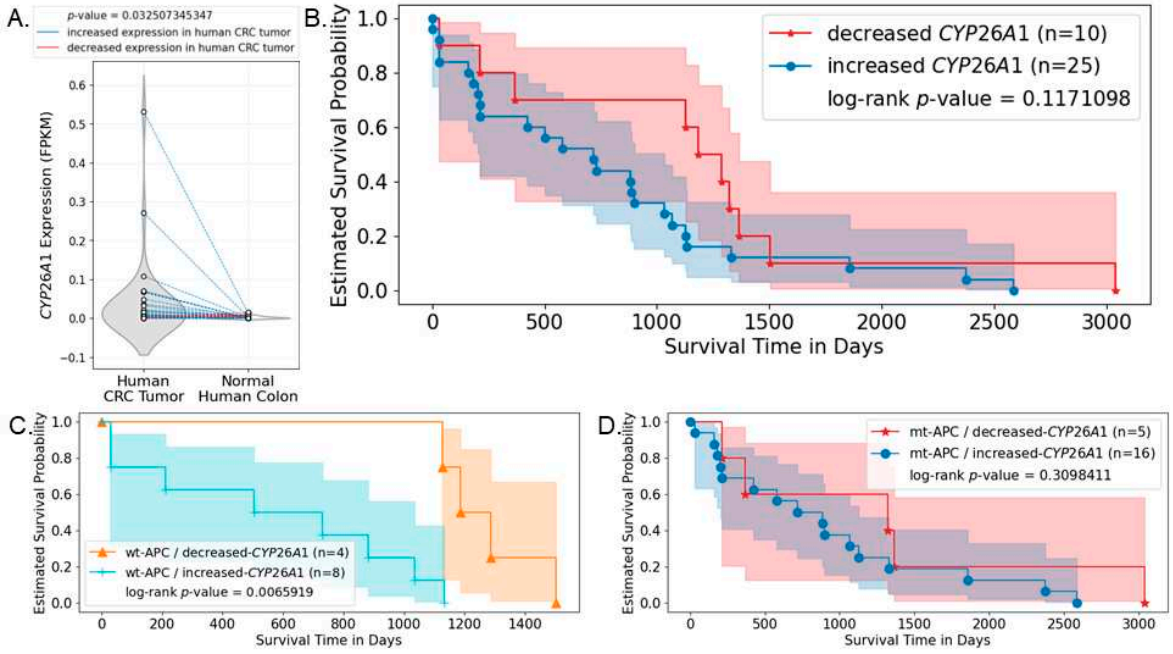

Figure 7. *CYP26A1* expression is a significant predictor of patient survival when patient tumors carry wild-type, but not mutant, *APC*. RNA-seq, mutation, and survival data of CRC patients were obtained from the GDC data portal and analyzed. (A) *CYP26A1* expression in both human CRC and normal human colon samples were plotted. Dots representing paired samples from the same patient are connected by lines. Particularly, blue lines indicate increased *CYP26A1* expression in human patient CRC samples compared to normal colon samples from the same patient; red lines indicate decreased expression of *CYP26A1* in human CRC samples compared to normal colon samples from the same patient. Shaded area indicates 95% confidence interval. Results show that the majority of CRC patients have increased expression of *CYP26A1* in their CRC samples compared to normal colon samples, and this increase is statistically significant. (B) This difference in *CYP26A1* expression level between CRC and normal colon sample is not a statistically significant predictor of patient survival. (C) When patients are additionally grouped based on whether they carry *APC* mutations or not, results show that change in *CYP26A1* expression between paired-tumor and normal samples is a significant predictor of patient survival only when their tumors carry *wt-APC*. (D) Such significance is not seen when patient tumors carry mutant *APC* (mt-*APC*).

 doi:10.20944/preprints202312.1224.v1

4. Discussion

We previously established that overpopulation of ALDH+ CSCs correlates with zygosity state of *APC* mutation during the stepwise tumor development in FAP patients [1]. We also found that *APC* mutation causes failure of ALDH+ SCs to mature into NECs [8,18]. Together, these findings provide a clue to a functional interaction between the WNT and RA signaling pathways that maintain stemness and promote differentiation, respectively [8,14,18]. Accordingly, we conjectured that a link exists between WNT and RA pathways, and, when *APC* is mutant, an imbalance in a WNT:RA-linked mechanism promotes CRC development [8]. Our main finding herein identified *CYP26A1* as a link between WNT and RA signaling that can be targeted to decrease ALDH+ SCs and increase retinoid-induced differentiation of *APC*-mutant CRC cells. The functional relevance of this finding is that 1) *CYP26A1* expression is controlled by WNT signaling via *APC* [30], and 2) *CYP26A1* enzyme controls intracellular RA metabolism and regulates RA signaling [16,17]. Our previous finding that RA signaling mainly occurs via ALDH+ SCs [14] raises two key questions addressed below:

Q1 *How is RA signaling regulated in ALDH+ SCs?*
Q2 *How does dysregulation of RA signaling due to APC mutation contribute to overpopulation of ALDH+ SCs that drives development of CRC?*

Studying the effect of wt-APC on ATRA response indicates that WNT signaling, via its target gene CYP26A1, regulates RA signaling in the differentiation of ALDH+ SCs.

We found that inducing *wt-APC* expression, which decreases WNT-signaling, reduced expression of several WNT target genes and increased sensitivity of HT29 cells to the anti-proliferative effects of ATRA (Figures 1 and S1). We also found that ATRA treatment of HT29 cells significantly increased *CYP26A1* expression (30.8-fold) and inducing *wt-APC* attenuated this increase by 50% (Figure 5A). This increase of *CYP26A1* by ATRA treatment of *APC* mutant HT29 cells may be explained by two factors 1) *CYP26A1* is a RA target gene [31–33] which should be induced by ATRA. 2) *CYP26A1* is also a WNT target gene [30] and ATRA increases WNT/β-catenin activity in HT29 cells even though they already have constitutively activated WNT due to mutated *APC* (Figure 1C). Notably, increased *CYP26A1* expression in ATRA treated HT29 cells decreases when they are induced to express wt-*APC* (Figure 5). This finding indicates that the ability of wt-*APC* to reduce WNT/β-catenin activity is the main mechanism that counterbalances the ability of ATRA to increase CYP26A1 expression. Consequently, since *wt-APC* inhibits WNT signaling, it should maintain the balance between WNT and RA signaling. Indeed, that is precisely what we observed because induction of *wt-APC* reversed ATRA's ability to increase: *i*) WNT/β-catenin activity (Figure 1C) and *ii*) *CYP26A1* expression (Figure 5). These findings show that modulation of *CYP26A1* levels by WNT signaling regulates RA signaling in *APC* mutant cells. Thus, our findings indicate that the anti-proliferative effect of ATRA is greatly enhanced by decreased expression of CYP26A1 due to the ability of wt-*APC* to reduce WNT signaling.

Since the RA pathway components are mainly expressed in ALDH+ SCs [14], WNT signaling, via its target gene *CYP26A1*, regulates RA signaling in ALDH+ SCs. Indeed, inducing *wt-APC* expression reduced expression of *CYP26A1* and enhanced the ability of ATRA to decrease CRC cell proliferation (Figures 1 and 5). Moreover, inducing *wt-APC*: *i*) suppressed ALDH1A1 expression, *ii*) decreased ALDH+ SCs, and *iii*) increased neuroendocrine cell differentiation. These findings show that *APC's* role in the control of WNT signaling regulates, via its target gene *CYP26A1*, RA signaling in the differentiation of ALDH+ CSCs.

To further explore the mechanism by which WNT signaling might regulate RA signaling, we examined differential mRNA expression in HT29 cells that were induced to express *wt-APC* and that were treated with ATRA compared to their respective controls. NanoString profiling revealed that among the 248 genes showing a significant change in expression, *CYP26A1* showed the greatest increase in expression (Figures 4C and S2). Additionally, our NanoString and bioinformatics analyses identified a novel CYP26A1-based network of protein interactions which reveals how WNT and RA pathways are inter-connected. Specifically, we found that a unique signaling cascade that links

Preprints (www.preprints.org) | NOT PEER-REVIEWED | Posted: 18 December 2023 doi:10.20944/preprints202312.1224.v1

components of the RA signaling pathway (CYP26A1, RARA) with components of the WNT pathway (DKK1, WNT7B, WNT11, FZD7) via HDAC2, KLF4, and TNF (Figure 4B). Thus, a CYP26A1-based network of both RA and WNT signaling components is predicted to play a role in the functional link between these two pathways.

Studying the effect of APC mutation on NEC differentiation indicates that decreased RA signaling contributes to overpopulation of ALDH+ SCs that drives development of CRC.

We found that inducing *wt-APC* expression, which decreases WNT-signaling and lowers *CYP26A1* expression, leads to a decrease in cell proliferation (Figure 1A,B) and an increase in NEC differentiation (Figures 2A,B and 3). Inducing *wt-APC* also decreased ALDH+ SC numbers and reduced expression of the ALDH1A1 SC marker (Figure 2C,D). Altogether, these findings show that elevated *CYP26A1* levels prevent differentiation of CSCs in *APC* mutant cells by increasing RA clearance which reduces RA signaling (Figure 8). This mechanism provides an explanation for how decreased RA signaling contributes to ALDH+ SCs overpopulation that drives CRC development.

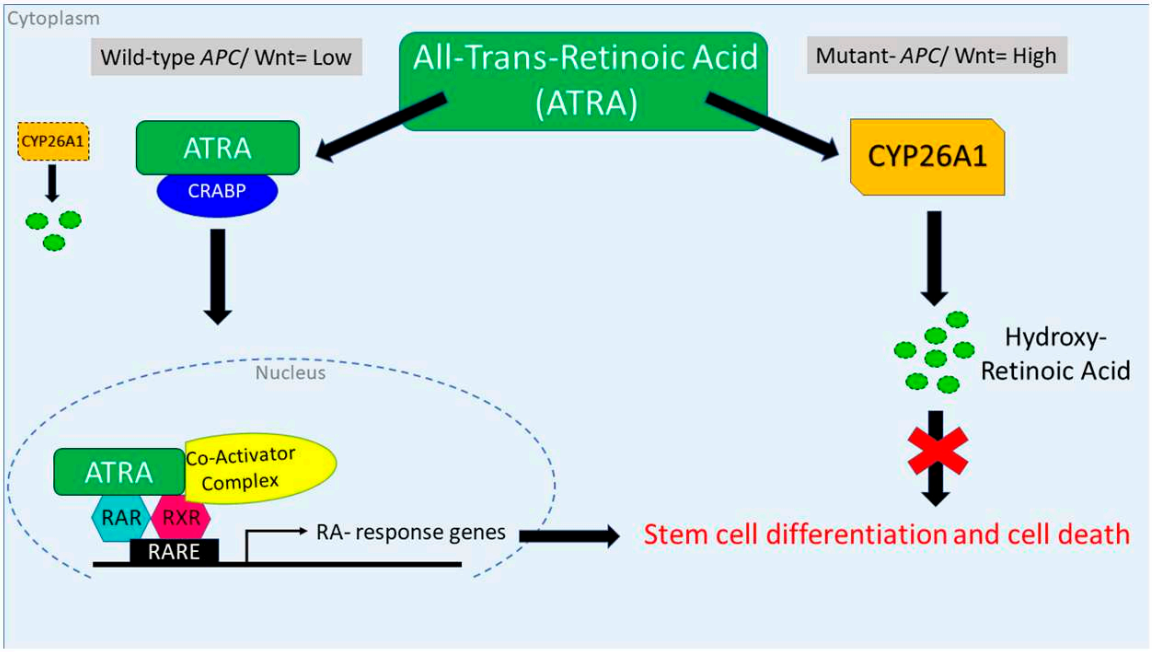

Figure 8. Attenuation of WNT signaling by induced *wt-APC* expression decreases *CYP26A1* and increases progression through the RA pathway. High WNT signaling levels correlate with a mutant *APC* genotype. In this case, when ATRA is administered, *CYP26A1* is overexpressed which increases metabolism of ATRA into hydroxy-retinoic acid, thereby preventing differentiation of SCs. When *wt-APC* expression is induced, components of the WNT signaling pathway, including *CYP26A1*, are not highly expressed. In this case, when ATRA is administered, it binds to CRABP to enter the nucleus and RA response genes are transcribed and then translated in the cytoplasm to allow differentiation of SCs and subsequent cell death.

Our results concur with the finding in Shelton et al [30] in which *CYP26A1* was upregulated in the intestine of *APC* mutant zebrafish embryos (and $Apc^{Min/+}$ mouse adenomas, human FAP adenomas, and human sporadic CRCs) but not in zebrafish embryos with *wt-APC*. Defects in gut differentiation was also reversed with pharmacologic inhibition or knockdown of *CYP26A1* in *APC* mutant zebrafish embryos [30]. Further studies on zebrafish showed that *APC* has a dual role in regulating Wnt and RA signaling [34,35]. Therefore, expression of *wt-APC* or pharmacologic inhibition of *CYP26A1* may provide a novel therapeutic strategy to sensitize CRC cells to ATRA [36]. For example, a recent study by Penny et al. involved treating $Apc^{Min/+}$ mice with the *CYP26A1* inhibitor Liarozole [37]. The administration of Liarozole to $Apc^{Min/+}$ mice increased endogenous RA signaling (by blocking ATRA metabolism), and dramatically reduced intestinal adenoma numbers in these

 doi:10.20944/preprints202312.1224.v1

Apc-mutant mice. We also found that the treatment of human CRC cells with Liarozole decreased proliferation, sphere formation, and the size of the ALDH+ SC population [14]. This suggests that decreasing the intracellular metabolism of ATRA using agents that inhibit CYP26A1 activity, might be a way to increase ATRA levels and therapeutically augment RA signaling in order to decrease CSC numbers in *APC*-mutant colon cancer tissues [16].

Clinical significance of our results that show CYP26A1 inhibitors, which block RA metabolism, sensitize CRC cells to anti-proliferative effect of drugs that downregulate WNT signaling.

Our findings likely have vast clinical importance. For instance, given that RA receptor mutant CRC cells show similar response to the *CYP26A1* inhibitors (Liarozole and Talarozole) as do non-mutant cells (Figure 6), this indicates that the inhibition of *CYP26A1* leads to a high enough intracellular RA level to induce growth inhibition regardless of RA receptor genotype. We then investigated the effects of these *CYP26A1* inhibitors in combination with agents (Sulindac or Piroxicam) that have anti-tumor activity against *APC*-mutant tissues and Sulindac is known to target β-catenin and downregulate WNT signaling [reviewed in 16]. Notably, when Sulindac or Piroxicam was combined with *CYP26A1* inhibitors Liarozole or Talarozole, the drug combination produced additive or synergistic effects (Figure 6C,F).

That the drug combinations reduce CRC proliferation to a greater extent than the *CYP26A1* inhibitors or anti-WNT agents alone indicates that inhibiting *CYP26A1* to increase RA signaling combined with the effect of inhibiting WNT signaling holds great promise as a therapeutic approach in oncology.

For human CRC cases, CYP26A1 predicts patient survival according to APC genotype.

Bioinformatics analysis of human CRC cases provides further evidence that *CYP26A1* has clinical significance (Figure 7). We found that the majority of CRC patients express an increased level of *CYP26A1* in their tumor tissues compared to normal colon from the same patient. Considering that *CYP26A1* is a key enzyme responsible for RA degradation, patients who express lower levels of *CYP26A1* should have higher levels of RA in their tumor cells, which should up-regulate RA-signaling activity and endow CRC patients with better survival. This prediction is supported by our results showing that *CYP26A1* is only a significant determinant of patient survival when patient tumors carry wild-type, but not mutant, *APC*. This finding also supports the existence of crosstalk between WNT and RA-signaling that is dependent upon *CYP26A1* expression level (hence cellular RA level), and *APC* genotype of the patients.

5. Conclusions

This work has vast clinical significance because it shows how CRC SCs might be sensitized to retinoid-induced cellular differentiation. We present a mechanism and therapeutic strategy to explain how differentiation-inducing agents such as ATRA may be used to promote CSC differentiation. Indeed, RA is an effective therapeutic agent in the treatment of acute promyelocytic leukemia (APL) [38–42]. RA therapy has also been shown to improve the survival of neuroblastoma patients [43]. While using retinoids to treat other cancers has shown limited success [16,17], therapeutically inhibiting CYP26A1, as we have shown herein, to reduce RA metabolism may prove useful in designing approaches to promote differentiation of CSCs with retinoids. Therefore, our findings are important because CRC development is driven by overpopulation of CSCs which are resistant to conventional chemotherapies and radiation [44–46]. Thus, finding ways to promote retinoid-induced differentiation of CSCs *in vivo* may lead to new and more effective therapeutic strategies for CRC patients.

Supplementary Materials: The following supporting information can be downloaded at the website of this paper posted on Preprints.org, Figure S1. WNT/β- catenin activity is reduced with expression of *wt-APC*. Figure S2. Inducing wild-type *APC* and treating with ATRA to drive RA signaling activates a highly regulated network of 248 proteins.

Author Contributions: Conceptualization, (BMB, COBF); methodology (COBF, LMO); software (COBF, BO, CZ); validation (COBF, LMO, VOH, BO, CZ); formal analysis (COBF, LMO, VOH, BO, CZ); investigation (COBF,

VOH, BO, CZ); resources (BMB, COBF, LMO); data curation (COBF, CZ); writing—original draft preparation (BMB, COBF); writing—review and editing (BMB, COBF, BO, CZ, VH); visualization (COBF); supervision (BBM); project administration (NBN, LMO); funding acquisition (BMB). All authors have read and agreed to the published version of the manuscript.

Funding: This study was supported in part by The Lisa Dean Moseley Foundation (2022; BMB, COBF, LMO), Cancer B*Ware Foundation (2018; BMB.), The Cawley Center for Translational Cancer Research Fund (2021; BMB, COBF, LMO), The Carpenter Foundation (BMB), University of Delaware Department of Biological Sciences (2021; VOH, BO, CZ) and INBRE NIH/NIGMS GM103446 (BMB).

Institutional Review Board Statement: Not applicable.

Informed Consent Statement: Not applicable.

Data Availability Statement: We encourage all authors of articles published in MDPI journals to share their research data. In this section, please provide details regarding where data supporting reported results can be found, including links to publicly archived datasets analyzed or generated during the study. Where no new data were created, or where data is unavailable due to privacy or ethical restrictions, a statement is still required. Suggested Data Availability Statements are available in section "MDPI Research Data Policies" at https://www.mdpi.com/ethics#_bookmark21.

Acknowledgments: We would like to thank Dr. Nicholas Petrelli for his support at the Helen F. Graham Cancer Center and Research Institute. We also thank the Vogelstein Lab at John's Hopkins University for providing the inducible *wt-APC* cell lines. Special thanks to Sandy Widura and Dr. Sonali Majumdar at the Wistar Institute for performing our NanoString profiling experiments. Thanks also to all members past and present of Dr. Boman's lab: Dr. Shirin Modarai, Victoria Stark, and Molly Lausten for their thoughtful discussions and contributions. Lastly, we acknowledge Dr. Ahui Ma and Dr. Jennifer Sims-Mourtada for their thoughtful discussions.

Conflicts of Interest: The authors declare no conflict of interest.

Abbreviations

CRC: colorectal cancer, ALDH: aldehyde dehydrogenase, SC: stem cell, CSC: cancer stem cell, ATRA: all-trans-retinoic acid, *APC*: adenomatous polyposis coli, wt: wild type, mt: mutant, WNT: Wingless and Int-1 signaling, *CYP26A1*: Cytochrome P450 Family 26 Subfamily A Member 1, RA = retinoic acid, NEC: neuroendocrine cell, DMSO: dimethyl sulfoxide, IC50: half-maximal inhibitory concentration.

References

1. Huang, E.H.; Hynes, M.J.; Zhang, T.; Ginestier, C.; Dontu, G.; Appelman, H.; Fields, J.Z.; Wicha, M.S.; Boman, B.M. Aldehyde Dehydrogenase 1 Is a Marker for Normal and Malignant Human Colonic Stem Cells (SC) and Tracks SC Overpopulation during Colon Tumorigenesis. *Cancer Res* 2009, *69*, 3382–3389. https://doi.org/10.1158/0008-5472.can-08-4418.
2. Boman, B.M.; Walters, R.; Fields, J.Z.; Kovatich, A.J.; Zhang, T.; Isenberg, G.A.; Goldstein, S.D.; Palazzo, J.P. Colonic Crypt Changes during Adenoma Development in Familial Adenomatous Polyposis. *Am J Pathol* 2004, *165*, 1489–1498. https://doi.org/10.1016/s0002-9440(10)63407-4.
3. Ma, I.; Allan, A.L. The Role of Human Aldehyde Dehydrogenase in Normal and Cancer Stem Cells. *Stem Cell Rev Rep* 2010, *7*, 292–306. https://doi.org/10.1007/s12015-010-9208-4.
4. Marchitti, S.A.; Brocker, C.; Stagos, D.; Vasiliou, V. Non-P450 Aldehyde Oxidizing Enzymes: The Aldehyde Dehydrogenase Superfamily. *Expert Opin Drug Metab Toxicol* 2008, *4*, 697–720. https://doi.org/10.1517/17425255.4.6.697.
5. M., A.; Bagirova, M.; Nehir, O.; Yaman, S.; Sefik, E.; Cakir, R.; Canim, S.; Elcicek, S.; Yesilkir, S. Aldehyde Dehydrogenase: Cancer and Stem Cells. In *Dehydrogenases*; InTech, 2012. https://doi.org/10.5772/48591.
6. Black, W.J.; Stagos, D.; Marchitti, S.A.; Nebert, D.W.; Tipton, K.F.; Bairoch, A.; Vasiliou, V. Human Aldehyde Dehydrogenase Genes: Alternatively Spliced Transcriptional Variants and Their Suggested Nomenclature. *Pharmacogenet Genomics* 2009, *19*, 893–902. https://doi.org/10.1097/fpc.0b013e3283329023.
7. Das, B.C.; Thapa, P.; Karki, R.; Das, S.; Mahapatra, S.; Liu, T.-C.; Torregroza, I.; Wallace, D.P.; Kambhampati, S.; Veldhuizen, P. Van; et al. Retinoic Acid Signaling Pathways in Development and Diseases. *Bioorg Med Chem* 2014, *22*, 673–683. https://doi.org/10.1016/j.bmc.2013.11.025.
8. Zhang, T.; Ahn, K.; Emerick, B.; Modarai, S.R.; Opdenaker, L.M.; Palazzo, J.; Schleiniger, G.; Fields, J.Z.; Boman, B.M. *APC* Mutations in Human Colon Lead to Decreased Neuroendocrine Maturation of ALDH+ Stem Cells That Alters GLP-2 and SST Feedback Signaling: Clue to a Link between WNT and Retinoic Acid

Signalling in Colon Cancer Development. *PLoS One* 2020, 15, e0239601. https://doi.org/10.1371/journal.pone.0239601.
9. Morin, P.J.; Vogelstein, B.; Kinzler, K.W. Apoptosis and *APC* in Colorectal Tumorigenesis. *Proc Natl Acad Sci USA* 1996, *93*, 7950–7954. https://doi.org/10.1073/pnas.93.15.7950.
10. Zhang, T.; Fields, J.Z.; Opdenaker, L.; Otevrel, T.; Masuda, E.; Palazzo, J.P.; Isenberg, G.A.; Goldstein, S.D.; Brand, M.; Boman, B.M. Survivin-Induced Aurora-B Kinase Activation. *Am J Pathol* 2010, *177*, 2816–2826. https://doi.org/10.2353/ajpath.2010.100047.
11. Zhang, T.; Otevrel, T.; Gao, Z.; Gao, Z.; Ehrlich, S.M.; Fields, J.Z.; Boman, B.M. Evidence That *APC* Regulates Survivin Expression: A Possible Mechanism Contributing to the Stem Cell Origin of Colon Cancer. *Cancer Res* 2001, *61*, 8664–8667.
12. Barker, N.; Ridgway, R.A.; van Es, J.H.; van de Wetering, M.; Begthel, H.; van den Born, M.; Danenberg, E.; Clarke, A.R.; Sansom, O.J.; Clevers, H. Crypt Stem Cells as the Cells-of-Origin of Intestinal Cancer. *Nature* 2008, *457*, 608–611. https://doi.org/10.1038/nature07602.
13. Dow, L.E.; O'Rourke, K.P.; Simon, J.; Tschaharganeh, D.F.; van Es, J.H.; Clevers, H.; Lowe, S.W. *APC* Restoration Promotes Cellular Differentiation and Reestablishes Crypt Homeostasis in Colorectal Cancer. *Cell* 2015, *161*, 1539–1552. https://doi.org/10.1016/j.cell.2015.05.033.
14. Modarai, S.R.; Gupta, A.; Opdenaker, L.M.; Kowash, R.; Masters, G.; Viswanathan, V.; Zhang, T.; Fields, J.Z.; Boman, B.M. The Anti-Cancer Effect of Retinoic Acid Signaling in CRC Occurs via Decreased Growth of ALDH Colon Cancer Stem Cells and Increased Differentiation of Stem Cells. *Oncotarget* 2018, *9*, 34658–34669. https://doi.org/10.18632/oncotarget.26157.
15. Clark, D.W.; Palle, K. Aldehyde Dehydrogenases in Cancer Stem Cells: Potential as Therapeutic Targets. *Ann Transl Med* 2016, *4*, 518. https://doi.org/10.21037/atm.2016.11.82.
16. Hunsu, V.O.; Facey, C.O.B.; Fields, J.Z.; Boman, B.M. Retinoids as Chemo-Preventive and Molecular-Targeted Anti-Cancer Therapies. *Int J Mol Sci* 2021, *22*, 7731. https://doi.org/10.3390/ijms22147731.
17. Facey COB, Boman BM. Retinoids in Treatment of Colorectal Cancer [Online First], *IntechOpen*. https://doi.org/10.5772/intechopen.93699. Available from: https://www.intechopen.com/online-first/retinoids-in-treatment-of-colorectal-cancerRetinoids in Treatment of Colorectal Cancer, IntechOpen 2020.
18. Modarai, S.R.; Opdenaker, L.M.; Viswanathan, V.; Fields, J.Z.; Boman, B.M. Somatostatin Signaling via SSTR1 Contributes to the Quiescence of Colon Cancer Stem Cells. *BMC Cancer* 2016, *16*, 941. https://doi.org/10.1186/s12885-016-2969-7.
19. Boman, B.M.; Fields, J.Z. An *APC*:WNT Counter-Current-Like Mechanism Regulates Cell Division Along the Human Colonic Crypt Axis: A Mechanism That Explains How *APC* Mutations Induce Proliferative Abnormalities That Drive Colon Cancer Development. *Front Oncol* 2013, *3*. https://doi.org/10.3389/fonc.2013.00244.
20. Https://Nanostring.Com/Products/Ncounter-Assays-Panels/Oncology/Ncounter-Pancancer-Pathways-Panel/.
21. Szklarczyk, D.; Kirsch, R.; Koutrouli, M.; Nastou, K.; Mehryary, F.; Hachilif, R.; Gable, A.L.; Fang, T.; Doncheva, N.T.; Pyysalo, S.; et al. The STRING Database in 2023: Protein–Protein Association Networks and Functional Enrichment Analyses for Any Sequenced Genome of Interest. *Nucleic Acids Res* 2023, *51*, D638–D646. https://doi.org/10.1093/nar/gkac1000.
22. Liu Q, Yin X, Languino LR, Altieri DC. Evaluation of drug combination effect using a Bliss independence dose-response surface model. *Stat Biopharm Res* 2018, *10*, 112-122. https://doi.org/10.1080/19466315.2018.1437071.
23. Http://Web.Stanford.Edu/Group/Nusselab/Cgi-Bin/Wnt/Target_genes.
24. Boon, E.M.J.; van der Neut, R.; van de Wetering, M.; Clevers, H.; Pals, S.T. Wnt Signaling Regulates Expression of the Receptor Tyrosine Kinase Met in Colorectal Cancer. *Cancer Res* 2002, *62*, 5126–5128.
25. Mann, B.; Gelos, M.; Siedow, A.; Hanski, M.L.; Gratchev, A.; Ilyas, M.; Bodmer, W.F.; Moyer, M.P.; Riecken, E.O.; Buhr, H.J.; et al. Target Genes of β-Catenin–T Cell-Factor/Lymphoid-Enhancer-Factor Signaling in Human Colorectal Carcinomas. *Proc Natl Acad Sci USA* 1999, *96*, 1603–1608. https://doi.org/10.1073/pnas.96.4.1603.
26. Wielenga, V.J.M.; Smits, R.; Korinek, V.; Smit, L.; Kielman, M.; Fodde, R.; Clevers, H.; Pals, S.T. Expression of CD44 in *APC* and Tcf Mutant Mice Implies Regulation by the WNT Pathway. *Am J Pathol* 1999, *154*, 515–523. https://doi.org/10.1016/S0002-9440(10)65297-2.
27. He, T.-C.; Sparks, A.B.; Rago, C.; Hermeking, H.; Zawel, L.; da Costa, L.T.; Morin, P.J.; Vogelstein, B.; Kinzler, K.W. Identification of C- MYC as a Target of the *APC* Pathway. *Science* 1998, *281*, 1509–1512. https://doi.org/10.1126/science.281.5382.1509.
28. Wiedenmann, B.; Franke, W.W.; Kuhn, C.; Moll, R.; Gould, V.E. Synaptophysin: A Marker Protein for Neuroendocrine Cells and Neoplasms. *Proc Natl Acad Sci USA* 1986, *83*, 3500–3504. https://doi.org/10.1073/pnas.83.10.3500.
29. Https://David.Ncifcrf.Gov/.

30. Shelton, D.N.; Sandoval, I.T.; Eisinger, A.; Chidester, S.; Ratnayake, A.; Ireland, C.M.; Jones, D.A. Up-Regulation of *CYP26A1* in Adenomatous Polyposis Coli-Deficient Vertebrates via a WNT-Dependent Mechanism: Implications for Intestinal Cell Differentiation and Colon Tumor Development. *Cancer Res* 2006, *66*, 7571–7577. https://doi.org/10.1158/0008-5472.CAN-06-1067.
31. Ozpolat B, Mehta K, Lopez-Berestein G. Regulation of a highly specific retinoic acid-4-hydroxylase (*CYP26A1*) enzyme and all-trans-retinoic acid metabolism in human intestinal, liver, endothelial, and acute promyelocytic leukemia cells. *Leuk Lymphoma* 2005 *46*, 1497-1506. https://doi.org/10.1080/10428190500174737. PMID: 16194896.
32. Balmer JE, Blomhoff R. Gene expression regulation by retinoic acid. *J Lipid Res* 2002 *43* 1773-808. https://doi.org/10.1194/jlr.r100015-jlr200. PMID: 12401878.
33. Rhinn M, Dollé P. Retinoic acid signalling during development. *Development* 2012 *139*, 843-58. https://doi.org/10.1242/dev.065938. PMID: 22318625.
34. Nadauld LD, Sandoval IT, Chidester S, Yost HJ, Jones DA. Adenomatous polyposis coli control of retinoic acid biosynthesis is critical for zebrafish intestinal development and differentiation. *J Biol Chem* 2004 *279*, 51581-9. https://doi.org/10.1074/jbc.M408830200.
35. Nadauld LD, Chidester S, Shelton DN, Rai K, Broadbent T, Sandoval IT, Peterson PW, Manos EJ, Ireland CM, Yost HJ, Jones DA. Dual roles for adenomatous polyposis coli in regulating retinoic acid biosynthesis and Wnt during ocular development. *Proc Natl Acad Sci USA* 2006 *103*, 13409-14. https://doi.org/10.1073/pnas.0601634103.
36. Nelson, C.; Buttrick, B.; Isoherranen, N. Therapeutic Potential of the Inhibition of the Retinoic Acid Hydroxylases *CYP26A1* and CYP26B1 by Xenobiotics. *Curr Top Med Chem* 2013, *13*, 1402-28. https://doi.org/10.2174/1568026611313120004.
37. Penny, H.L.; Prestwood, T.R.; Bhattacharya, N.; Sun, F.; Kenkel, J.A.; Davidson, M.G.; Shen, L.; Zuniga, L.A.; Seeley, E.S.; Pai, R.; et al. Restoring Retinoic Acid Attenuates Intestinal Inflammation and Tumorigenesis in *Apc*Min/ Mice. *Cancer Immunol Res* 2016, *4*, 917–926. https://doi.org/10.1158/2326-6066.cir-15-0038.
38. Idres, N.; Benoıˆt, G.; Flexor, M.A.; Lanotte, M.; Chabot, G.G. Granulocytic Differentiation of Human NB4 Promyelocytic Leukemia Cells Induced by All-Trans Retinoic Acid Metabolites. *Cancer Res* 2001, *61*, 700-5.
39. Zhu, J.-W.; Shi, X.G.; Chu, H.Y.; Tong, J.H.; Wang, Z.; Naoe, T.; Waxman, S.M.; Chen, S.; Chen, Z. Effect of retinoic acid isomers on proliferation, differentiation and PML relocalization in the APL cell line NB4. *Leukemia* 1995, *9*, 302–309.
40. Fang, J.; Chen, S.-J.; Tong, J.-H.; Wang, Z.-G.; Chen, G.-Q. Treatment of Acute Promyelocytic Leukemia with ATRA and As2O3: A Model of Molecular. *Cancer Biol Ther* 2002, *1*, 614–620. https://doi.org/10.4161/cbt.308.
41. Yilmaz, M.; Kantarjian, H.; Ravandi, F. Acute Promyelocytic Leukemia Current Treatment Algorithms. *Blood Cancer J* 2021, *11*, 123. https://doi.org/10.1038/s41408-021-00514-3.
42. Stahl, M.; Tallman, M.S. Acute Promyelocytic Leukemia (APL): Remaining Challenges towards a Cure for ALL. *Leuk Lymphoma* 2019, *60*, 3107–3115. https://doi.org/10.1080/10428194.2019.1613540.
43. Gudas, L.J.; Wagner, J.A. Retinoids Regulate Stem Cell Differentiation. *J Cell Physiol* 2011, *226*, 322-30. https://doi.org/10.1002/jcp.22417.
44. Phi, L.T.H.; Sari, I.N.; Yang, Y.-G.; Lee, S.-H.; Jun, N.; Kim, K.S.; Lee, Y.K.; Kwon, H.Y. Cancer Stem Cells (CSCs) in Drug Resistance and Their Therapeutic Implications in Cancer Treatment. *Stem Cells Int* 2018 Feb 28;2018:5416923. https://doi.org/10.1155/2018/5416923.
45. Prieto-Vila, M.; Takahashi, R.; Usuba, W.; Kohama, I.; Ochiya, T. Drug Resistance Driven by Cancer Stem Cells and Their Niche. *Int J Mol Sci* 2017, *18*, 2574. https://doi.org/10.3390/ijms18122574.
46. Boman, B.M.; Wicha, M.S. Cancer Stem Cells: A Step Toward the Cure. *J Clin Oncol* 2008, *26*, 2795–2799. https://doi.org/10.1200/JCO.2008.17.7436.